Stable and Tunable Current-Induced Phase Transition in Epitaxial Thin Films of Ca_2RuO_4

*Atsushi Tsurumaki-Fukuchi,**,† *Keiji Tsubaki*,† *Takayoshi Katase,*‡ *Toshio Kamiya,*‡ *Masashi Arita*,† *and Yasuo Takahashi*†

† Graduate School of Information Science and Technology, Hokkaido University, Kita-14, Nishi-9, Kita-Ku, Sapporo 060-0814, Japan

‡ Laboratory for Materials and Structures, Institute of Innovative Research, Tokyo Institute of Technology, 4259 Nagatsuta-cho, Midori-ku, Yokohama 226-8503, Japan

KEYWORDS: metal-insulator transition, ruthenium oxide, epitaxial thin film, current-induced transition, solid-phase epitaxy, resistive switching

ABSTRACT: Owing to the recent discovery of the current-induced metal-insulator transition and unprecedented electronic properties of the concomitant phases of calcium ruthenate Ca_2RuO_4, it is emerging as an important material. To further explore the properties, the growth of epitaxial thin films of Ca_2RuO_4 is receiving more attention as high current densities can be applied to thin-film samples and the amount can be precisely controlled in an experimental environment. However, it is difficult to grow high-quality thin films of Ca_2RuO_4 due to easy formation of crystal defects originating from sublimation of RuO_4; therefore, the metal-insulator transition of Ca_2RuO_4 is typically not observed in the thin films. Herein, stable current-induced metal-insulator transition is achieved in high-quality thin films of Ca_2RuO_4 grown by solid phase epitaxy under high growth temperatures and pressures. In the Ca_2RuO_4 thin films grown by ex-situ annealing at >1200 °C and 1.0 atm, continuous changes in the resistance of over two orders of magnitude are induced by currents with a precise dependence of the resistance on the current amplitude. A hysteretic, abrupt resistive transition is also observed in the thin films from the resistance–temperature measurements conducted under constant-voltage (variable-current) conditions with a controllability of the transition temperature. A clear resistive switching by the current-induced transition is demonstrated in the current–electric-field characteristics, and the switching currents and fields are shown to be very stable. These results represent a significant step toward understanding the high-current-density properties of Ca_2RuO_4 and future development of Mott-electronic devices based on electricity-driven transitions.

INTRODUCTION

As an important unsolved problem in strongly correlated electron physics, the possibility of electricity-driven metal-insulator transition, where the current density or electric field serves as the control parameter, has been actively debated since the 1990s.[1,2] Moreover, to enable the practical application of Mott memories and transistors,[3] current- and field-induced metal-insulator transition has been intensively explored in recent years due to their significant advantages in electronics applications. Easier integrability into electronic devices and higher controllability of the resistance state is expected for the electricity-induced transition than the more general temperature-induced metal-insulator transition,[4,5] as it can be operated purely by electrical parameters, and not by temperature increases through Joule heating. Recent studies have successfully verified the presence of electrically driven transitions in some narrow-gap Mott insulators,[6–13] and these materials are receiving increasing attention. Layered perovskite Ca_2RuO_4 (CRO) is one such material, where the metal-insulator transition is induced by currents or fields through electron redistributions in the 4*d* t_{2g} orbitals.[9,10,13–16] In CRO, novel electronic properties that do not appear in the thermally induced phases have been observed in the electrically induced phases, including strong diamagnetism under a high current density.[13] This indicates the particular importance of the electricity induced transitions of CRO because the electrically driven transitions in other materials generally induces only the same phases with the thermally driven transitions. Therefore, active investigations into the electronic properties of CRO are being conducted, particularly for the high-current-density phases.

The characterization of epitaxial thin films is considered essential for understanding the mechanisms of the electrically induced transition of CRO as the current density of thin films can be precisely controlled and much increased under experimental conditions. However, previous

studies have demonstrated that the metal-insulator transition of CRO becomes very obscure in the thin films.[17–20] Gradual temperature-dependent changes in the resistivity ρ have been observed over a broad temperature range of 2–300 K in the thin films, instead of the sharp transition in bulk CRO. The low-temperature ρ of the CRO thin films is also strongly dependent on the growth method with approximate values of 10^{-3} Ω cm by pulsed laser deposition (PLD)[17–19] and 10^{-1} Ω cm by molecular beam epitaxy (MBE).[20] However, the transport properties of thin-film ruthenates are strongly influenced by the high concentrations of crystallographic (planer and point) defects.[21–25] In CRO thin films, the large influence of crystal defects is also suggested from the growth method dependence of ρ. The superconductivity of thin films of strontium ruthenate Sr_2RuO_4, which is a chemical analog of CRO with a similar crystal structure, has recently been achieved by reducing the planar defects and Ru deficiencies.[23–25] This suggests that the suppression of crystallographic defects may influence the observations of the metal-insulator transition of CRO thin films and allow for a detailed understanding of electrically induced transitions. Therefore, in this study, we attempted to grow epitaxial thin films of CRO with a reduced defect density and achieve electrically driven transition in the films.

Here, we demonstrate stable current-induced transition in epitaxial thin films of CRO grown by solid phase epitaxy (SPE). To suppress defect formation in CRO thin films, we performed epitaxial growth at a high temperature above 1200 °C under a non-vacuum pressure of 1.0 atm by SPE. As previous studies on Sr_2RuO_4 thin films[24,25] demonstrated that utilizing a high growth temperature and preventing the composition loss of Ru due to the sublimation of RuO_4 in the vacuum deposition[26] are vital for defect suppression, we assumed that the high growth temperatures and pressures of the SPE method would aid in high-quality epitaxial growth of CRO. In the CRO thin films grown by SPE, clear current-induced transition was observed in the resistance–temperature

(*R*–*T*) and current–electric-field (*I*–*E*) characteristics. The switching-currents and fields of the transition were extremely stable. Additionally, we found that the behavior of the current-induced transition can be tuned based on the amount of current flow: Both gradual and abrupt resistive transitions are possible in the epitaxial films of CRO.

RESULTS AND DISCUSSION

In this study, CRO thin films with a thickness of 30 nm were grown on $LaAlO_3$ (LAO) (001) substrates, which had an AlO_2-terminated step-and-terrace surface formed by HCl etching.[27] The CRO thin films were grown from the amorphous precursor deposited on the LAO substrates, under an Ar + O_2 atmosphere with a pressure of 1.0 atm and temperature of 1200–1400 °C using an external furnace by SPE (see METHODS for details). The electrical transport measurements for the CRO thin films were conducted following standard four- and two-probe methods after applying Au(35 nm)/Cr(5 nm) electrodes to the films. The four-probe measurements were performed for large scale (>5.0 mm^2) samples using non-continuous reading currents of <50 μA. The two-probe method was used to investigate the current-induced transition. In the measurements, continuous currents or voltages were locally applied to the CRO thin films using two-terminal electrodes with a separation of 20 μm (see Figure S1 for details), fabricated on CRO thin films with a dimension of 1.0 × 1.0 cm^2.

The X-ray diffraction (XRD) patterns of the films in the θ–2θ scan (Figure 1a) indicated that phase-pure, *c*-axis-oriented thin films of CRO were grown by the SPE method. The in-plane orientations of the CRO films ([110] of CRO || [100] of LAO) were also confirmed from the ϕ scan

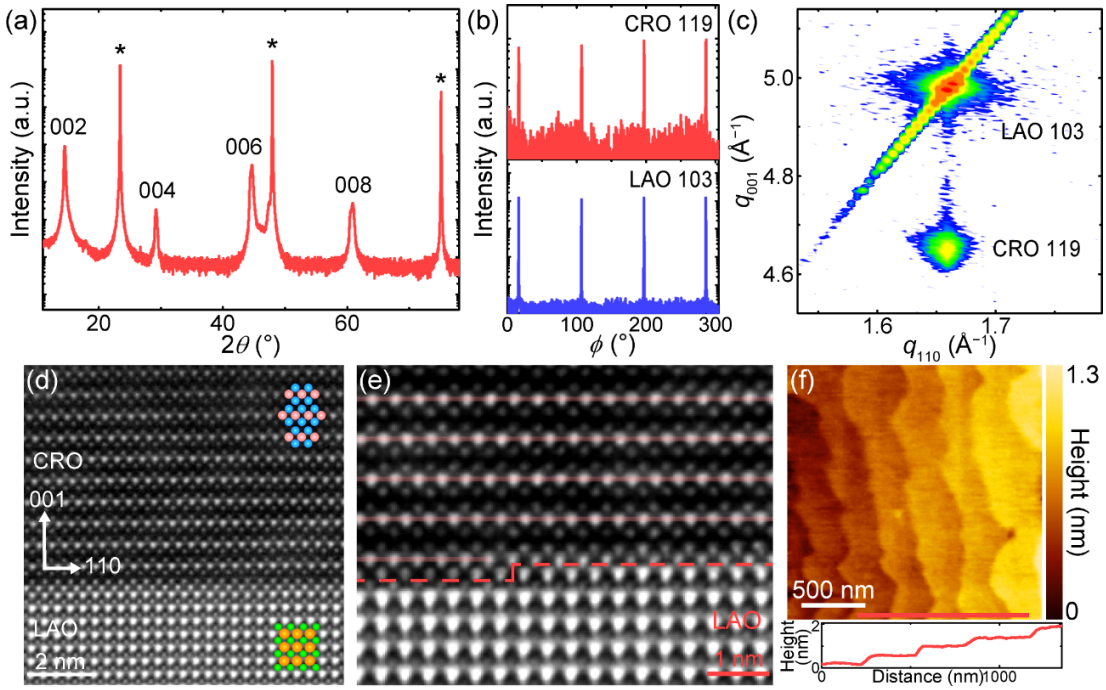

Figure 1. XRD patterns of a CRO thin film on an LAO (001) substrate grown by SPE, measured under (a) θ–2θ scan and (b) ϕ scan for the CRO 119 and LAO 103 reflections. The asterisks in (a) indicate the reflections from the LAO substrate. (c) Reciprocal space map around the CRO 119 and LAO 103 reflections obtained from XRD measurements. (d) Cross-sectional HAADF-STEM image of a CRO thin film grown on an LAO (001) substrate. The positions of Ca, Ru, La, and Al ions are indicated with blue, red, orange, and green spheres for clarity, respectively. (e) Higher-magnification HAADF-STEM image of a CRO film around a single-unit-cell-height step on the LAO substrate. The solid pink and broken red lines indicate the RuO_2 planes of CRO and CRO/LAO interface, respectively. (f) Topographic AFM image of a CRO thin film on an LAO (001) substrate. The bottom figure shows the surface profile along the horizontal red line in the image.

(Figure 1b). The reciprocal space mapping by XRD (Figure 1c) indicated that the in-plane crystal lattice of the CRO film is matched with that of the LAO substrate, and the lattice constants were $a = b = 0.536$ nm and $c = 1.216$ nm. These values indicate that the crystal lattice of the CRO film is elongated from that of bulk CRO in the *c*-axis direction, which has $a = 0.541$ nm, $b = 0.549$ nm, and $c = 1.196$ nm at $T = 295$ K,[28] due to compressive strain from LAO (with amounts of 0.9–2.4%). The *c*-axis lattice constant of the SPE-grown thin films was slightly smaller than the lattice constant *c* of approximately 1.224 nm reported for CRO/LAO (001) thin films grown by PLD.[18,19] The smaller lattice constant may indicate the reduced defect densities of the SPE-grown thin films, as the lattice constants of ruthenate thin films generally increase with increasing defect concentrations.[29]

The coherent growth of the CRO films and a sharp interface structure were also observed in the high-angle annular dark-field (HAADF) images obtained by scanning transmission electron microscopy (STEM) (Figure 1d). In the TEM observations, few extended defects were detected in the CRO lattice over ~300 nm width. In previous studies on epitaxial thin films of CRO and Sr_2RuO_4, out-of-phase boundaries (OPBs) were assumed to be inevitably formed in the films particularly at the surface steps of the substrate with an approximate height of 0.4 nm[19,24,30] (Figure S2a and b). However, in our thin films grown at high temperatures, OPB formation was significantly suppressed, even at the steps on the substrate. As shown in Figure 1e, structural mismatch in the out-of-plane direction was immediately accommodated in the first unit cell of CRO at most of the substrate steps (see Figure S2b for details). Atomic force microscopy (AFM) observations indicated that the CRO films had a periodic surface structure with atomically flat terraces and 0.4 nm-high steps (Figure 1f). This structure indicates that the "steric type" of OPBs[30] in the film were formed at these steps with an approximate interval of 300 nm, which was much

smaller than the step interval on the LAO substrate (Figure S2a), and were accommodated by the CRO lattice. Unaccommodated OPBs were also observed in the TEM observations (Figure S2c) with an approximate interval of 300 nm, and were the only notable defects observed.

The in-plane resistivity ρ of the CRO thin films exhibited an insulator-like temperature dependence in $T = 4$–400 K (Figure 2a), and the values were much lower than those of bulk CRO.[31] The reduced ρ is considered due to the destabilization of the insulating phase by the compressible strain from the LAO substrates.[19] Similar insulator-like behavior of ρ has also been reported in CRO/LAO (001) thin films grown by MBE,[20] however, the values in the SPE-grown films are one to two orders of magnitude higher than those of MBE-grown films. The large growth-method dependence of ρ suggests the strong influence of the crystal defects on the metal-insulator transition of CRO thin films. Three possible mechanisms can be envisioned for the influences: (a) hole doping by Ru deficiency formation, (b) electron doping by O deficiency formation, and (c) changes in the structural-stress state by defect formation. While further investigations are necessary to identify the dominant mechanism, the difference of ρ between the SPE- and MBE-grown thin films can be explained by the changes in the structural stresses as a possible scenario. Our SPE-grown thin films were shown to have a smaller *c*-axis lattice constant of 1.216 nm than that of PLD grown thin films (1.224 nm).[18,19] This indicates that the SPE-grown thin films will have a smaller compressive strain in the in-plane direction due to reduction of the defect-induced lattice expansion.[29] Therefore, anisotropic in-plane pressure effects on the metal-insulator transition[32] will be reduced in the SPE-grown thin films, and the ρ will be increased.

The Hall resistivity ρ_{xy} of the SPE-grown thin films exhibited an almost linear dependence on the magnetic field up to 9 T (Figure 2b). The majority carriers in the CRO films were indicated to

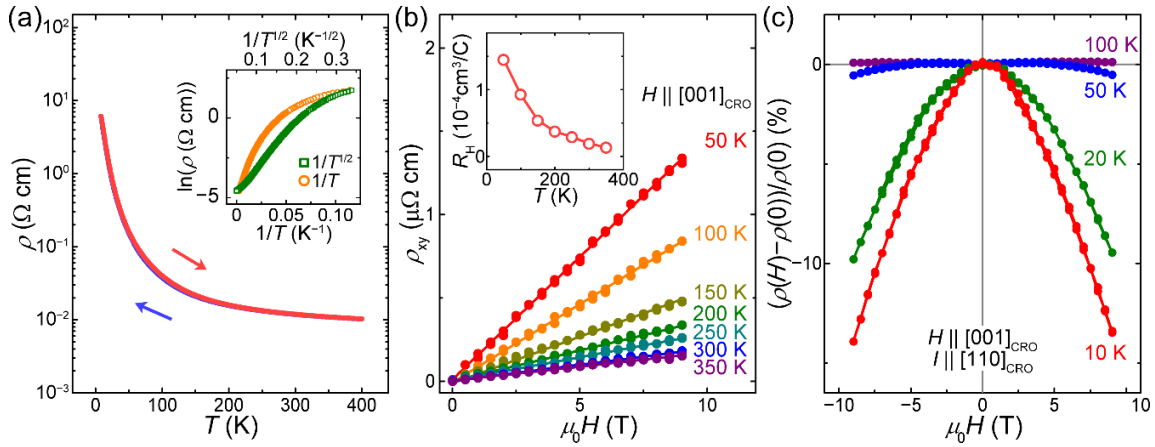

Figure 2. (a) Temperature dependence of the in-plane ρ for a CRO thin film on an LAO (001) substrate grown by SPE. The inset shows ln(ρ) vs. $1/T$ and $1/T^{1/2}$ plots for the ρ–T characteristic. (b) Magnetic field dependence of the Hall resistivity ρ_{xy} and (c) in-plane magnetoresistance for a CRO thin film on an LAO (001) substrate measured at T = (b) 50–350 K and (c) 10–100 K. The inset in (b) shows the temperature dependence of the R_H derived from the ρ_{xy} measurements.

be holes, based on the positive Hall coefficients R_H (inset of Figure 2b) determined from the slopes of the ρ_{xy}–H characteristics. The carrier concentrations derived from the R_H were 4.3×10^{22} cm^{-3} at 50 K and 1.7×10^{23} cm^{-3} at 200 K. These concentrations are much increased from those of bulk CRO (3.5×10^{16} cm^{-3} at 200 K).[33] Effects of the compressive epitaxial strain of 0.9–2.4% from the LAO substrate will be involved in the increased carrier concentrations. The in-plane compression will inhibit flattening distortion of RuO_6 octahedra in CRO lattice, which causes energy splitting between the ($4d_{xz}$, $4d_{yz}$) and $4d_{xy}$ orbitals,[34] and will stabilize the metallic phases as observed in bulk CRO under uniaxial[32] and chemical[34] pressures. However, the very small values of R_H may be due to the nonnegligible contributions from the minority carriers (electrons)

and suggest the occurrence of mixed conduction by holes and electrons in the CRO thin films. The R_H of the CRO thin films was highly dependent on the temperature (inset of Figure 2b). Such strong temperature dependence of R_H has been observed in bulk metallic $(Ca,Sr)_2RuO_4$[35] and CRO in current applications,[13] often with a temperature-dependent reversal of the sign, indicating the alteration of the carrier type. However, in our CRO thin films, no sign reversal was observed for the R_H in the temperature range of 50–350 K. For the current-induced phases of bulk CRO, negative magnetoresistance of approximately −2% at 7 T was also observed.[13] Regarding this feature, our CRO thin films exhibited large negative magnetoresistance, even before applying a large constant current. As shown in Figure 2c, the CRO thin film begun to exhibit negative magnetoresistance below an approximate temperature T of 50 K, and the value reached to −9% at $\mu_0 H$ = 7 T and T = 10 K. This behavior may suggest that the magnetic ground state of the CRO thin films is ferromagnetic, as such large negative magnetoresistance is generally caused by the spin fluctuation in a ferromagnetic material, which has been observed in bulk CRO under isotropic pressure.[36]

In bulk CRO, the temperature dependence of ρ fits well the activation-type insulating behavior of $\ln(\rho) \propto T^{-1}$ or the Efros-Shklovskii-type variable-range hopping mechanism of $\ln(\rho) \propto T^{-1/2}$ in $T < 250$ K.[10,31,37] The ρ of bulk CRO deviates from these laws near the metal-insulator transition temperature T_M of 357 K due to the supposed changes in the energy gap and effective mass.[10] In our CRO thin films, however, the ρ deviated from these dependences in the all range of T = 4–400 K (inset of Figure 2a). We have confirmed that the temperature dependence of ρ also does not obey small-polaron or Mott-variable-range hopping mechanisms. The temperature-dependences of ρ and R_H suggest that the metal-insulator transition of the CRO films was broadened over this temperature range due to the epitaxial strain from LAO, similarly to

CRO/LAO (001) thin films grown by PLD.[18,19] The SPE-grown films are supposed to be in a metastable state below the T_M of 240 K (as discussed later), where the transition is not completely undergone.

Current-induced resistive transition was found to emerge when applying continuous currents to the CRO thin films using a two-terminal gap electrode (Figure S1). In the resistance–temperature characteristics measured under a constant current flow, gradual suppressions of the resistance were observed depending on the current amplitude (Figure 3a). We observed that this current-dependent resistance change was a reversible phenomenon. By reducing the applied currents after the application of 10 mA, very similar *R*–*T* characteristics were measured under the lower current amplitudes. The current dependence of the resistance almost disappeared above a ridge observed at 240 K (Figures 3a and S3). This temperature can be considered as the T_M of the SPE-grown CRO films, from which the broadened transition begins. This T_M is close to that of CRO/LAO (001) thin films grown by MBE (T_M = 230 K).[20] The coincidence of the T_M in the SPE- and MBE-grown films also suggests that their difference in the ρ is mainly caused by the difference in the in-plane strain, which does not cause an apparent shift in the T_M.[32] Regarding the *I*–*E* characteristics measured with the same electrode, a rapid increase in the currents (i.e., resistive switching) and hysteretic behavior were observed when the temperature was approximately 60 K or less after reaching a threshold current I_{th} of 8.7 mA (Figure 3b). This current value corresponds to a current density of around 0.4 MA cm^{-2} in the electrode configuration (Figure S1). Little temperature dependence was observed in I_{th}, whereas the threshold field E_{th}, which is the electric field under which resistive switching occurs, exhibited a systematic variation depending on temperature.

Additionally, we found that an abrupt phase transition emerges in the CRO thin films by

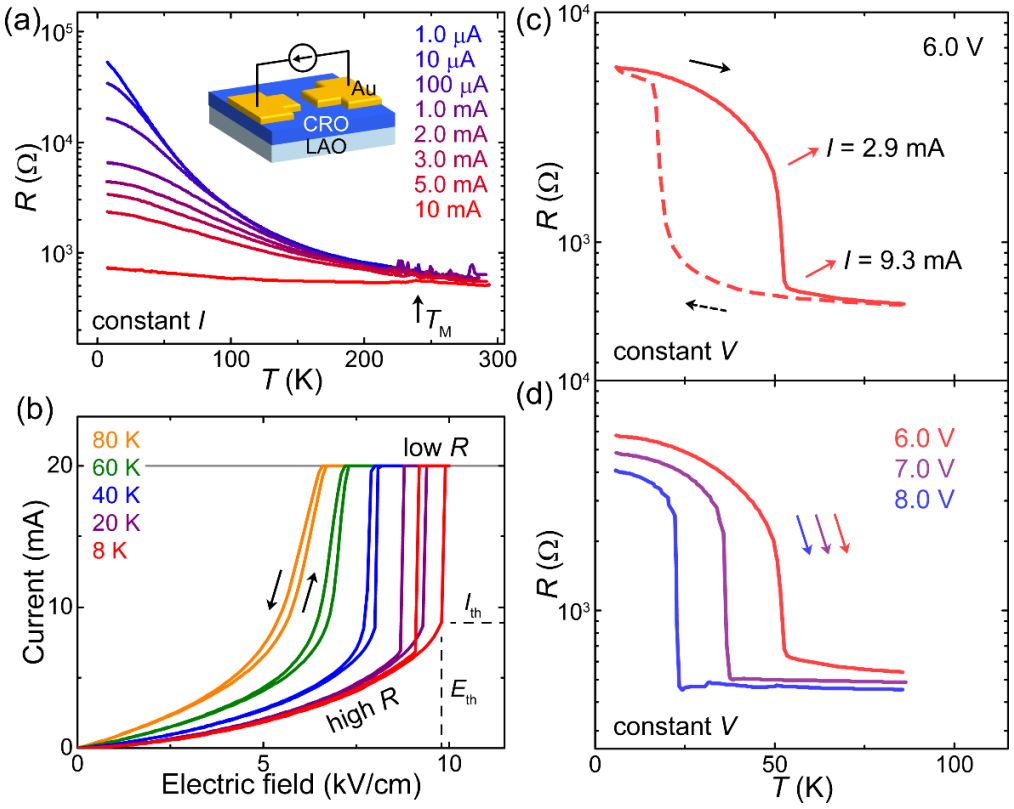

Figure 3. (a) Temperature dependence of the resistance of a CRO thin film on an LAO (001) substrate measured under a constant current of 1.0 μA–10 mA. The inset is a schematic illustration of the two-terminal electrode with a lateral gap of 20 μm used for the measurements. (b) *I*–*E* characteristics of a CRO thin film on an LAO (001) substrate measured at $T = 8$–80 K. The arrows indicate the directions of the electric field sweeping. The horizontal line at 20 mA shows the current compliance set by the measurement unit. (c) Temperature dependence of the resistance of a CRO thin film on an LAO (001) substrate measured under a constant voltage of 6.0 V, and (d) its voltage-amplitude dependence. The current values shown in (c) are for the two representative data points before/after the rapid change in the resistance was observed.

conducting measurements under constant-voltage conditions (i.e., with no current limit; Figure 3c). The abrupt transition exhibited hysteresis due to temperature sweeping, which is typical of first-order metal-insulator transitions. Regarding the heating characteristic, a rapid increase in the currents (from 2.9 to 9.3 mA) was observed before and after the transition, which is consistent with the constant-current-mode measurements (Figure 3a), where the resistance was largely suppressed in a similar range of currents. We also observed that the temperature of the abrupt resistive transition can be tuned by the voltage amplitudes. As shown in Figure 3d, the transition temperature was significantly shifted depending on the voltage, with an amount of approximately 20 K/V.

For single crystals of bulk CRO, cracking (sample break-down) is readily caused by current- and field-induced transition due to the large deformation in the crystal structure.[9] However, the breakdown problem was significantly suppressed in the epitaxial thin films discussed here, and stable cycling of the current-induced transition was achieved. Figure 4a presents the results of the *I–E* measurements under multiple field sweeping cycles. The characteristics followed very similar profiles during the 15 sweeping cycles, and the switching to the low resistance state occurred at the same E_{th} between 9.6–9.7 kV cm^{-1}. The polarity reversal of the applied fields also caused no change in the *I–E* characteristics (Figure 4b). The cycle-to-cycle distributions of I_{th} and E_{th} in the CRO thin films appeared to be significantly smaller than those in threshold switching by temperature-induced metal-insulator transition, where distributions of >10% typically occur due to the randomness in the Joule heating and thermal dissipation.[38,39] We examined the influences of thermal dissipation on the *I–E* characteristics of the CRO thin films by changing the field sweeping rate. In the measurements shown in Figure 4c, the field sweeping rate was changed by setting a waiting time (t_w) for every measurement point having a measurement period of 10 points/kV cm^{-1}.

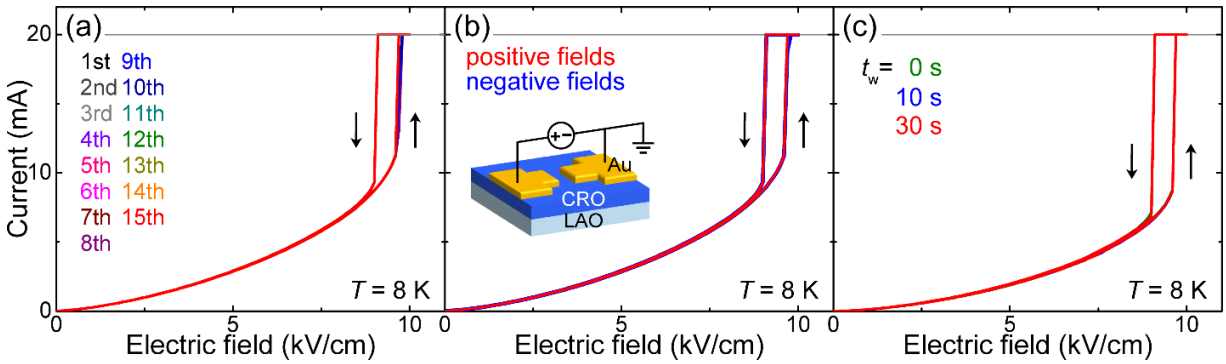

Figure 4. *I–E* characteristics of CRO thin films on LAO (001) substrates measured at $T = 8$ K for (a) 15 field sweeping cycles, (b) two cycles with different voltage polarities, and (c) three cycles with different sweeping rates controlled by the t_w. Note that two different samples were used for the measurements shown in (a,b) and (c), respectively. The arrows in the figures indicate the directions of the electric field sweeping. The horizontal lines at 20 mA show the current compliance set by the measurement unit.

Because the amount of heat generated by Joule heating and thermal dissipation has a time dependence, the E_{th} of resistive switching by temperature-induced metal-insulator transition strongly depends on the field sweeping rate.[38] The two-terminal structures used for the measurements were shown to be in non-thermal equilibrium at $t_w = 0$ s from the current hysteresis observed at an increased temperature (Figure S4), and the local temperatures will also have a time dependence in the measurements. However, the I_{th} and E_{th} of the CRO thin films did not change with the field sweeping rate, and the *I–E* characteristics were stable (Figure 4c).

The measurements also indicate that the *I–E* characteristics are highly nonlinear in the field range before the abrupt switching occurs. We have confirmed that the characteristics do not fit an

exponential-type dependence, which is attributable to the interface barriers (data not shown). This suggests that the current-induced resistance suppression (Figure 3a) may have already been induced in the CRO films in the measurements, even before the abrupt switching is observed, and the upward curves are due to the decrease in the resistance. The suppressions of resistance observed by current applications of ≤5 mA in the *R*–*T* characteristics (Figure 3a) also support this conclusion.

The influences of increases in temperature due to Joule heating will be nonnegligible in the current transport of the CRO thin films as the current density in the measurements should be high (in the order of 0.1 MA cm^{-2}). However, the abrupt transition observed in the *I*–*E* and constant-voltage-mode measurements is unlikely to be explained by a local temperature increase in the samples, as the CRO thin films intrinsically have a gradual temperature dependence of ρ and there was no abrupt transition in the ρ–*T* curves (Figure 2a). However, an abrupt resistance–temperature slope is required for inducing resistive switching by Joule-heating-driven metal-insulator transitions.[4,5,40] Joule heating was also confirmed to not be the dominant cause of the transition from the resistance hysteresis observed in the *R*–*T* characteristics across T_M (see Figure S3 in the Supporting Information). In previous studies on Mott insulators, Zener[2] and avalanche[7] breakdowns of the Mott-Hubbard gap were proposed as possible origins of the electrically driven metal-insulator transition. However, in the CRO thin films, these field-driven mechanisms cannot explain the gradual current dependence of the resistance (Figure 3a), as they should cause threshold-like (two-state) changes in the resistance.

According to the above, the results suggest that the intrinsic control parameter of the observed transition is current (specifically current density), rather than electrical field or temperature. In bulk CRO, two possible scenarios have been proposed for the mechanism of the current-induced

transition and resistance changes by it. One is the current-dependent reduction of the Mott-Hubbard gap with the increase of occupancy of the $4d_{xz}$ and $4d_{yz}$ orbitals,[10] and the other is the gradual growth of the metallic domains depending on the current densities.[14] For our results, both phenomena can qualitatively explain the gradual and abrupt resistance changes observed in the CRO thin films based on the increases in the currents. However, some physical properties of the current-induced transition of the CRO thin films largely varied from those of bulk CRO, such as E_{th} (10 kV cm^{-1} versus 40 V cm^{-1})[9] and R_H ($+10^{-4}$ cm^3/C versus $\pm 10^3$ cm^3/C).[13] For a more precise description of the transition, future studies should conduct detailed investigations into the impacts of epitaxial strain and current densities.

CONCLUSIONS

In conclusion, current-induced phase transition was successfully demonstrated in high-quality epitaxial thin films of CRO grown by the SPE method. An abrupt resistive transition with a hysteretic behavior was observed in the *R*–*T* characteristics measured under constant-voltage conditions. The current-induced transition in the thin films exhibited very small variations in the switching fields and currents during cycling. High controllability of the resistance values and transition behaviors was also observed depending on the amplitudes of applied currents and voltages. These results also raised some questions concerning the mechanisms of the current-induced transition, such as the influences of the epitaxial strain and current densities. Although much higher current densities (~0.1 MA cm^{-1}) will be applied to the CRO thin films than those to bulk CRO (~1 A cm^{-1}),[13,15,16] qualitatively similar behaviors were observed between the transitions. To answer these questions, further measurements under controlled current densities via

micropatterning for the CRO thin films should be conducted. The findings in this study will open new areas for controlling strongly correlated electronic phases based on current applications, and future developments of Mott-electronic devices with high controllability of the resistance state.

METHODS

Thin-Film Growth. During the first step of SPE growth of CRO thin films, amorphous precursor films with a composition of $Ca_2Ru_{1+x}O_{4+y}$ were deposited on LAO (001) substrates by PLD. Sintered mixtures of $CaCO_3$ and RuO_2 with a final nominal composition of $Ca_2Ru_{1.5}O_{4+y}$ were used as the PLD targets. The deposition was performed in a vacuum PLD chamber at room temperature with an oxygen partial pressure of 10 Pa using a KrF excimer laser (λ = 248 nm) with a fluence of ~2 J cm^{-1} and repetition rate of 10 Hz. The surfaces of the LAO (001) substrates were etched with concentrated HCl solutions prior to deposition to form an atomically stepped structure. The precursor films were then annealed in an external tube furnace for 1.0 h at T = 1200–1400 °C under an Ar(99%) + O_2(1%) atmosphere and a pressure of 1.0 atm to complete the epitaxial growth of CRO. In this article, CRO thin films annealed at T = 1350 °C were used for the measurements, where the best crystallinity was obtained.

Structure Characterization. The crystal structures and orientations of the films were investigated by XRD measurements using a SmartLab (Rigaku) and D8 Discover (Bruker AXS Inc.) with a Cu Kα source, and TEM using a JEM-ARM200F (JEOL) after focused ion-beam milling with a Quanta 3D 200i (Thermo Fisher Scientific). The surface morphologies of the films were observed by AFM using a NanoCute (Hitachi High-Tech Co.).

Electrical characterization. Au(35 nm)/Cr(5 nm) electrodes were fabricated on the CRO thin films by vacuum evaporation and photolithography to capture the electrical measurements. The four-probe resistivity, Hall effect, and magnetoresistance measurements were carried out in the physical property measurement system (PPMS, Quantum Design). The two-probe resistance was measured with a system consisting of a cryocooler, multimeter (Keithley 2002), and direct current source (Yokogawa 7651). The *I–E* characteristics were measured using a Keysight 4156C Semiconductor Parameter Analyzer and a cryogenic probe station (Nagase, GRAIL-20-305-6-LV).

ASSOCIATED CONTENT

Supporting Information

The Supporting Information is available free of charge at .

Optical microscope images of the electrode configuration; STEM image of an OPB; detailed resistance–temperature characteristics across T_M; and current–electric-field characteristics at an increased temperature (PDF)

AUTHOR INFORMATION

Corresponding Author

Atsushi Tsurumaki-Fukuchi − *Graduate School of Information Science and Technology, Hokkaido University, Kita-14, Nishi-9, Kita-Ku, Sapporo 060-0814, Japan*; orcid.org/0000-0003-2529-8897; Email: a.fukuchi@ist.hokudai.ac.jp

Authors

Keiji Tsubaki − *Graduate School of Information Science and Technology, Hokkaido University, Kita-14, Nishi-9, Kita-Ku, Sapporo 060-0814, Japan*

Takayoshi Katase − *Laboratory for Materials and Structures, Institute of Innovative Research, Tokyo Institute of Technology, 4259 Nagatsuta-cho, Midori-ku, Yokohama 226-8503, Japan*; orcid.org/0000-0002-2593-7487

Toshio Kamiya − *Laboratory for Materials and Structures, Institute of Innovative Research, Tokyo Institute of Technology, 4259 Nagatsuta-cho, Midori-ku, Yokohama 226-8503, Japan*

Masashi Arita − *Graduate School of Information Science and Technology, Hokkaido University, Kita-14, Nishi-9, Kita-Ku, Sapporo 060-0814, Japan*

Yasuo Takahashi − *Graduate School of Information Science and Technology, Hokkaido University, Kita-14, Nishi-9, Kita-Ku, Sapporo 060-0814, Japan*

Complete contact information is available at:

Notes

The author declare no competing financial interest.

ACKNOWLEDGMENTS

This work was financially supported by the Japan Society for the Promotion of Science (JSPS, KAKENHI Nos 19K04484, 16K18073, and 16H04339) organized by the Ministry of Education, Culture, Sports and Technology (MEXT) Japan and the Hattori-Hokokai Foundation. Part of this work was conducted under the Nanotechnology Platform (Hokkaido Univ. and Kyushu Univ.) by MEXT and the Collaborative Research Projects of Laboratory for Materials and Structures,

Institute of Innovative Research, Tokyo Institute of Technology. The authors would like to thank Prof. Hiromichi Ohta (Hokkaido Univ.) for his helpful discussions and comments.

REFERENCES

(1) Asamitsu, A.; Tomioka, Y.; Kuwahara, H.; Tokura, Y. Current Switching of Resistive States in Magnetoresistive Manganite. *Nature* **1997**, *388*, 50–52.

(2) Oka, T.; Arita, R.; Aoki, H. Breakdown of a Mott Insulator: A Nonadiabatic Tunneling Mechanism. *Phys. Rev. Lett.* **2003**, *91*, 066406.

(3) Zhou, Y.; Ramanathan, S. Mott Memory and Neuromorphic Devices. *Proc. IEEE* **2015**, *103*, 1289–1310.

(4) Kumar, S.; Pickett, M. D.; Strachan, J. P.; Gibson, G.; Nishi, Y.; Williams, R. S. Local Temperature Redistribution and Structural Transition during Joule-Heating-Driven Conductance Switching in VO_2. *Adv. Mater.* **2013**, *25*, 6128–6132.

(5) Li, D.; Sharma, A. A.; Gala, D. K.; Shukla, N.; Paik, H.; Datta, S.; Schlom, D. G.; Bain, J. A.; Skowronski, M. Joule Heating-Induced Metal–Insulator Transition in Epitaxial VO_2/TiO_2 Devices. *ACS Appl. Mater. Interfaces* **2016**, *8*, 12908–12914.

(6) Cario, L.; Vaju, C.; Corraze, B.; Guiot, V.; Janod, E. Electric-Field-Induced Resistive Switching in a Family of Mott Insulators: Towards a New Class of RRAM Memories. *Adv. Mater.* **2010**, *22*, 5193–5197.

(7) Guiot, V.; Cario, L.; Janod, E.; Corraze, B.; Phuoc, V. T.; Rozenberg, M.; Stoliar, P.; Cren, T.; Roditchev, D. Avalanche Breakdown in $GaTa_4Se_{8-x}Te_x$ Narrow-Gap Mott Insulators. *Nat. Commun.* **2013**, *4*, 1722.

(8) Stoliar, P.; Cario, L.; Janod, E.; Corraze, B.; Guillot-Deudon, C.; Salmon-Bourmand, S.; Guiot, V.; Tranchant, J.; Rozenberg, M. Universal Electric-Field-Driven Resistive Transition in Narrow-Gap Mott Insulators. *Adv. Mater.* **2013**, *25*, 3222–3226.

(9) Nakamura, F.; Sakaki, M.; Yamanaka, Y.; Tamaru, S.; Suzuki, T.; Maeno, Y. Electric-Field-Induced Metal Maintained by Current of the Mott Insulator Ca_2RuO_4. *Sci. Rep.* **2013**, *3*, 2536.

(10) Okazaki, R.; Nishina, Y.; Yasui, Y.; Nakamura, F.; Suzuki, T.; Terasaki, I. Current-Induced Gap Suppression in the Mott Insulator Ca_2RuO_4. *J. Phys. Soc. Jpn.* **2013**, *82*, 103702.

(11) Hollander, M. J.; Liu, Y.; Lu, W.-J.; Li, L.-J.; Sun, Y.-P.; Robinson, J. A.; Datta, S. Electrically Driven Reversible Insulator–Metal Phase Transition in 1T-TaS_2. *Nano Lett.* **2015**, *15*, 1861–1866.

(12) Yoshida, M.; Suzuki, R.; Zhang, Y.; Nakano, M.; Iwasa, Y. Memristive Phase Switching in Two-Dimensional 1T-TaS_2 Crystals. *Sci. Adv.* **2015**, *1*, e1500606.

(13) Sow, C.; Yonezawa, S.; Kitamura, S.; Oka, T.; Kuroki, K.; Nakamura, F.; Maeno, Y. Current-Induced Strong Diamagnetism in the Mott Insulator Ca_2RuO_4. *Science* **2017**, *358*, 1084–1087.

(14) Zhang, J.; McLeod, A. S.; Han, Q.; Chen, X.; Bechtel, H. A.; Yao, Z.; Corder, S. N. G.; Ciavatti, T.; Tao, T. H.; Aronson, M.; Carr, G. L.; Martin, M. C.; Sow, C.; Yonezawa, S.; Nakamura, F.; Terasaki, I.; Basov, D. N.; Millis, A. J.; Maeno, Y.; Liu, M. Nano-Resolved Current-Induced Insulator-Metal Transition in the Mott Insulator Ca_2RuO_4. *Phys. Rev. X* **2019**, *9*, 011032.

(15) Bertinshaw, J.; Gurung, N.; Jorba, P.; Liu, H.; Schmid, M.; Mantadakis, D. T.; Daghofer, M.; Krautloher, M.; Jain, A.; Ryu, G. H.; Fabelo, O.; Hansmann, P.; Khaliullin, G.; Pfleiderer,

C.; Keimer, B.; Kim, B. J. Unique Crystal Structure of Ca_2RuO_4 in the Current Stabilized Semimetallic State. *Phys. Rev. Lett.* **2019**, *123*, 137204.

(16) Cirillo, C.; Granata, V.; Avallone, G.; Fittipaldi, R.; Attanasio, C.; Avella, A.; Vecchione, A. Emergence of a Metallic Metastable Phase Induced by Electrical Current in Ca_2RuO_4. *Phys. Rev. B* **2019**, *100*, 235142.

(17) Wang, X.; Xin, Y.; Stampe, P. A.; Kennedy, R. J.; Zheng, J. P. Epitaxial Thin Film Growth of $Ca_2RuO_{4+\delta}$ by Pulsed Laser Deposition. *Appl. Phys. Lett.* **2004**, *85*, 6146–6148.

(18) Miao, L.; Silwal, P.; Zhou., X.; Stern, I.; Peng, J.; Zhang, W.; Spinu, L.; Mao, Z.; Kim, D. H. Itinerant Ferromagnetism and Geometrically Suppressed Metal-Insulator Transition in Epitaxial Thin Films of Ca_2RuO_4. *Appl. Phys. Lett.* **2012**, *100*, 052401.

(19) Dietl, C.; Sinha, S. K.; Christiani, G.; Khaydukov, Y.; Keller, T.; Putzky, D.; Ibrahimkutty, S.; Wochner, P.; Logvenov, G.; van Aken, P. A.; Kim, B. J.; Keimer, B. Tailoring the Electronic Properties of Ca_2RuO_4 via Epitaxial Strain. *Appl. Phys. Lett.* **2018**, *112*, 031902.

(20) Chang, C. S.; Holtz, M.; Nair, H.; Ruf, J.; Shen, K.; Schlom, D.; Muller, D. Direct Imaging of Tilt Relaxation from the Interface in Epitaxially Strained Ca_2RuO_4 Thin Films using ABF-STEM. *Microsc. Microanal.* **2018**, *24*, 64–65.

(21) Zurbuchen, M. A.; Jia, Y.; Knapp, S.; Carim, A. H.; Schlom, D. G.; Zou, L.-N.; Liu, Y. Suppression of Superconductivity by Crystallographic Defects in Epitaxial Sr_2RuO_4 Films. *Appl. Phys. Lett.* **2001**, *78*, 2351–2353.

(22) Zurbuchen, M. A.; Jia, Y.; Knapp, S.; Carim, A. H.; Schlom, D. G.; Pan, X. Q. Defect Generation by Preferred Nucleation in Epitaxial $Sr_2RuO_4/LaAlO_3$. *Appl. Phys. Lett.* **2003**, *83*, 3891–3893.

(23) Krockenberger, Y.; Uchida, M.; Takahashi, K. S.; Nakamura, M.; Kawasaki, M.; Tokura, Y. Growth of Superconducting Sr_2RuO_4 Thin Films. *Appl. Phys. Lett.* **2010**, *97*, 082502.

(24) Uchida, M.; Ide, M.; Watanabe, H.; Takahashi, K. S.; Tokura, Y.; Kawasaki, M. Molecular Beam Epitaxy Growth of Superconducting Sr_2RuO_4 Films. *APL Mater.* **2017**, *5*, 106108.

(25) Nair, H. P.; Ruf, J. P.; Schreiber, N. J.; Miao, L.; Grandon, M. L.; Baek, D. J.; Goodge, B. H.; Ruff, J. P. C.; Kourkoutis, L. F.; Shen, K. M.; Schlom, D. G. Demystifying the Growth of Superconducting Sr_2RuO_4 Thin Films. *APL Mater.* **2018**, *6*, 101108.

(26) Shin, J.; Kalinin, S. V.; Lee, H. N.; Christen, H. M.; Moore, R. G.; Plummer, E. W.; Baddorf, A. P. Surface Stability of Epitaxial $SrRuO_3$ Films. *Surf. Sci.* **2005**, *581*, 118–132.

(27) Ohnishi, T.; Takahashi, K.; Nakamura, M.; Kawasaki, M.; Yoshimoto, M.; Koinuma, H. A-Site Layer Terminated Perovskite Substrate: $NdGaO_3$. *Appl. Phys. Lett.* **1999**, *74*, 2531–2533.

(28) Braden, M.; André, G.; Nakatsuji, S.; Maeno, Y. Crystal and Magnetic Structure of Ca_2RuO_4: Magnetoelastic Coupling and the Metal-Insulator Transition. *Phys. Rev. B* **1998**, *58*, 847–861.

(29) Ohnishi, T.; Takada, K. Epitaxial Thin-Film Growth of $SrRuO_3$, $Sr_3Ru_2O_7$, and Sr_2RuO_4 from a $SrRuO_3$ Target by Pulsed Laser Deposition. *Appl. Phys. Express* **2011**, *4*, 025501.

(30) Zurbuchen, M. A.; Tian, W.; Pan, X. Q.; Fong, D.; Streiffer, S. K.; Hawley, M. E.; Lettieri, J.; Jia, Y.; Asayama, G.; Fulk, S. J.; Comstock, D. J.; Knapp, S.; Carim, A. H.; Schlom, D. G. Morphology, Structure, and Nucleation of Out-of-Phase Boundaries (OPBs) in Epitaxial Films of Layered oxides. *J. Mater. Res.* **2007**, *22*, 1439–1471.

(31) Alexander, C. S.; Cao, G.; Dobrosavljevic, V.; McCall, S.; Crow, J. E.; Lochner, E.; Guertin, R. P. Destruction of the Mott Insulating Ground State of Ca_2RuO_4 by a Structural Transition. *Phys. Rev. B* **1999**, *60*, R8422–R8425.

(32) Taniguchi, H.; Nishimura, K.; Ishikawa, R.; Yonezawa, S.; Goh, S. K.; Nakamura, F.; Maeno, Y. Anisotropic Uniaxial Pressure Response of the Mott Insulator of Ca_2RuO_4. *Phys. Rev. B* **2013**, *88*, 205111.

(33) Nishina, Y.; Okazaki, R.; Yasui, Y.; Nakamura, F.; Terasaki, I. Anomalous Thermoelectric Response in an Orbital-Ordered Oxide Near and Far from Equilibrium. *J. Phys. Soc. Jpn.* **2017**, *86*, 093707.

(34) Anisimov, V. I.; Nekrasov, I. A.; Kondakov, D. E.; Rice, T. M.; Sigrist, M. Orbital-Selective Mott-Insulator Transition in $Ca_{2-x}Sr_xRuO_4$. *Eur. Phys. J. B* **2002**, *25*, 191–201.

(35) Galvin, L. M.; Perry, R. S.; Tyler, A. W.; Mackenzie, A. P.; Nakatsuji, S.; Maeno, Y. Hall Effect in Single Crystal $Ca_{2-x}Sr_xRuO_4$. *Phys. Rev. B* **2001**, *63*, 161102(R).

(36) Nakamura, F.; Nakai, R.; Takemoto, T.; Sakaki, M.; Suzuki, T.; Alireza, P. L.; Nakatsuji, S.; Maeno, Y. Anisotropic Giant Magnetoresistance near the Mott Transition in Pressurized Ca_2RuO_4. *Phys. Rev. B* **2009**, *80*, 193103.

(37) Nakatsuji, S.; Dobrosavljević, V.; Tanasković, D.; Minakata, M.; Fukazawa, H.; Maeno, Y. Mechanism of Hopping Transport in Disordered Mott Insulators. *Phys. Rev. Lett.* **2004**, *93*, 146401.

(38) Lee, S. B.; Kim, K.; Oh, J. S.; Kahng, B.; Lee, J. S. Origin of Variation in Switching Voltages in Threshold-Switching Phenomena of VO_2 thin films. *Appl. Phys. Lett.* **2013**, *102*, 063501.

(39) Beaumont, A.; Leroy, J.; Orlianges, J.-C.; Crunteanu, A. Current-Induced Electrical Self-Oscillations across Out-of-Plane Threshold Switches Based on VO_2 Layers Integrated in Crossbars Geometry. *J. Appl. Phys.* **2014**, *115*, 154502.

(40) Yamasaki, S.; Kanki, T.; Manca, N.; Pellegrino, L.; Marré, D.; Tanaka, H. Metal–Insulator Transition in Free-Standing VO_2/TiO_2 Microstructures through Low-Power Joule Heating. *Appl. Phys. Express* **2014**, *7*, 023201.

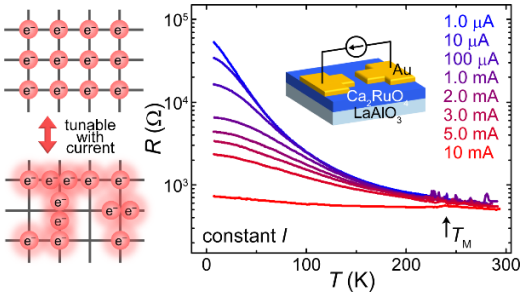

For Table of Contents Only